

1-1-1981

# Conduction Band Symmetry in Ta Chalcogenides from Ta L Edge X-ray Absorption Spectroscopy (XAS)

Juana Vivó Acrivos  
*San Jose State University*, juana.acrivos@sjsu.edu

S.S. P. Parkin  
*University of Cambridge*

J. Code  
*San Jose State University*

J. Reynolds  
*San Jose State University*

K. Hathaway  
*San Jose State University*

*See next page for additional authors*

Follow this and additional works at: [https://scholarworks.sjsu.edu/chem\\_pub](https://scholarworks.sjsu.edu/chem_pub)

 Part of the [Physical Chemistry Commons](#)

## Recommended Citation

Juana Vivó Acrivos, S.S. P. Parkin, J. Code, J. Reynolds, K. Hathaway, H. Kurasaki, and E. Marseglia. "Conduction Band Symmetry in Ta Chalcogenides from Ta L Edge X-ray Absorption Spectroscopy (XAS)" *Journal of Physics C: Solid State Physics* (1981): L349-L357. doi:10.1088/0022-3719/14/11/014

---

**Authors**

Juana Vivó Acivos, S.S. P. Parkin, J. Code, J. Reynolds, K. Hathaway, H. Kurasaki, and E. Marseglia

LETTER TO THE EDITOR

Conduction band symmetry in Ta chalcogenides from  
Ta L edge x-ray absorption spectroscopy (XAS)

J V Acrivos†, S S P Parkin‡, J Code†, J Reynolds†, K Hathaway†,  
H Kurasaki† and E A Marseglia‡

† San Jose State University, San Jose, CA 95912, USA

‡ Cavendish Laboratory, University of Cambridge, Madingley Road, Cambridge CB3  
001E, UK

Received 4 February 1981

**Abstract.** We report measurements of the x-ray absorption spectra near the Ta L edges of different polytypes of TaS<sub>2</sub> and TaSe<sub>2</sub> and TaSe<sub>3</sub>. Analysis of structure seen near the absorption edges and associated with transitions from well defined core levels to conduction band states has enabled the extent of the p character of the predominantly d character conduction band to be probed. The results show that the conduction band in the Ta chalcogenides studies has a significant amount of p character, and a lower limit of between 6 and 10% has been determined. The amount of p character varies between the various compounds in the following way:

$$1T\text{-TaS}_2 < \text{TaSe}_3 < 2H\text{-TaS}_2 \sim 1T\text{-TaSe}_2 < 2H\text{-TaSe}_2.$$

The Ta x-ray absorption edges have also been monitored during and after intercalation of the chalcogenides with hydrazine. Small changes in p character are observed and the results indicate that intercalation modifies the conduction band, not only through charge transfer, but more significantly through changes in hybridisation of the band.

In the layered transition metal dichalcogenides (TMDC) there is a long standing question concerning the extent of hybridisation of the metal d states with the chalcogen p states in the formation of the conduction band (schematic energy band structures for these compounds are given in Bell and Liang (1976); for a recent review of band structure calculations see, for example, Doran (1980) and references therein). Direct experimental data on the amount of hybridisation would be useful in the calculation of band structures of these materials, and in a fundamental understanding of those properties which depend on the bonding between the metal and chalcogen atoms. For example, the amount of hybridisation affects the interpretation of certain features in the measured reflectivity spectra of the group V(a) TMDC (Parkin and Beal 1980) and of excitonic features seen in the spectra of some of the group VI(a) dichalcogenides (Goldberg *et al* 1975).

Identification of the symmetry allowed transitions can be complicated in the visible-ultraviolet region because of the convolution of the valence band density of states (DOS) with the conduction band DOS on which the transition strength depends (see, for example, Liang and Beal 1976) and in the soft x-ray region because of overlap of transitions from different core levels. In particular, the XAS measurements of Sonntag

and Brown (1974) on  $2H-NbSe_2$ , in the soft x-ray region, are complicated by the overlap of the Se ( $M_V$  and  $M_{IV}$ ) and Nb ( $N_I$ ) edges at 56.7 and 58.1 eV respectively, although Sonntag and Brown have identified the strong absorption near 53–59 eV as resulting from Se  $M_V$ ,  $M_{IV}$  core level transitions to the conduction band states.

We have made measurements of the x-ray absorption spectra at the tantalum L edges ( $L_I$  at 11.68;  $L_{II}$  at 11.11;  $L_{III}$  at 9.88 keV) of different polytypes of  $TaS_2$  and  $TaSe_2$  and  $TaSe_3$ , in order to shed light on the symmetry of the conduction band states in these materials. (Note that the Ta L edges are well separated in energy from the Se K edge near 12.65 keV). XAS measures transitions from narrow core levels in the crystal to states in the conduction band and to the continuum. By observing the strengths of these transitions, information can be obtained directly about the symmetry of the states in the conduction band, because the absorption coefficient is related to the simple product of the conduction band density of states  $N_c(E)$  and the transition probability  $|M(E)|^2$ . If the conduction band consists of hybridised states of d and p symmetry then the selection rules for transitions will be modified accordingly and this will affect the strength of the transition. The symmetry allowed transitions between atomic levels on a single atom are as follows: (i) from the  $L_{III}$  edge,  $p_{3/2} \rightarrow d$  and  $s$ ; (ii) from the  $L_{II}$  edge,  $p_{1/2} \rightarrow d$  and  $s$ ; and (iii) from the  $L_I$  edge,  $s \rightarrow p$ .

The Ta L edges were measured at the Stanford Synchrotron Radiation Laboratory (SSRL) using procedures described elsewhere (see for example Lindau and Winick 1976 and Winick and Brown 1978). The photon fluxes used in these experiments were produced by the SPEAR storage ring running at 2 GeV and between 8 and 14 mA. The SSRL source with the experimental configuration used for this study is shown in figure 1. The crystalline samples were contained in an evacuated cell made from s/s 316 with 0.03" thick beryllium windows. A mask with an aperture smaller than the size of the

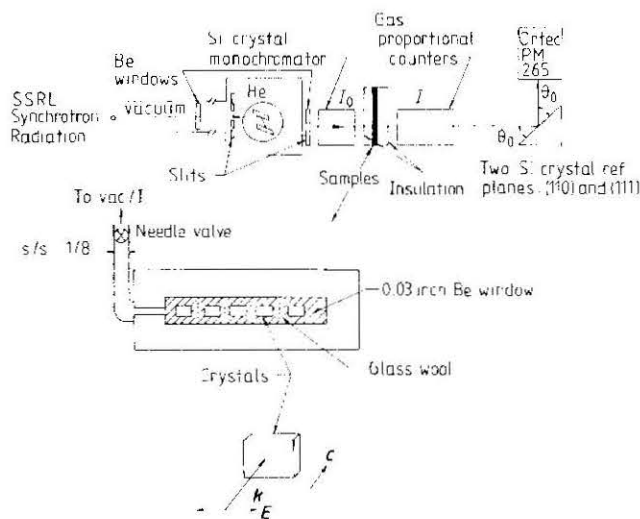


**Figure 1.** Schematic diagram of the experimental set-up, showing the SSRL synchrotron radiation source, silicon crystal monochromator and gas proportional counters, placed either side of the samples. Glass wool was used to hold the samples in place within an evacuated stainless steel cell containing beryllium windows, transparent in the energy range of interest. Bragg reflections from two silicon crystals cut along the (111) and (110) planes were used to determine accurately an energy reference marker for each scan, as described by Acrivos *et al* (1980).

Edge

 $L_I$  $L_{II}$  $L_{III}$ 

smallest crystal (app beam and each crystal absorbance at a part cleaving the single crystal ratio of incident to transmitted intensity  $A \equiv \ln(I_0/I) \sim 2-3$ , coefficients near the L edges. The x-ray beam from the propagation vector  $k$  and the crystal structure and the extent of the sample. In these experiments  $TaS_2$  or  $TaSe_2$  layers were better than 0.7 eV, with resolution of the L edges of a particular symmetry elements (Parratt 1954)  $\sim 6$  eV for the  $L_{III}$  lines have a similar resolution of the experiments, so (of total width  $\sim 7$  eV) in the soft x-ray region the resolution is about 0.2 eV; but the absorption spectrum is more complex.

The applicability of the theory at these energies has been examined by the refractive index  $n = 1 - \delta + i\epsilon$  and both  $\delta$  and  $\epsilon$  are near the x-ray absorption edges that  $\tilde{n}$  and  $\tilde{\epsilon}$  are given

$$\tilde{n} \equiv 1 - \delta$$

and

$$\tilde{\epsilon} \equiv \epsilon$$

If interference effects are neglected and the incident light parallel to the surface

$$T(E) =$$

**Table 1.** Tantalum mass absorption coefficients near the L edges in elemental tantalum, taken from the Chemical Rubber Company (CRC) handbook.

Edge	$\alpha_a^0$ (g cm <sup>-2</sup> )	$\Delta\alpha_a^0$ (g cm <sup>-2</sup> )
L <sub>I</sub>	262	43
L <sub>II</sub>	248	70
L <sub>III</sub>	246	149

smallest crystal (approximately 4 mm<sup>2</sup> in cross section) was placed across the incident beam and each crystal was located with translational step motors so as to maximise the absorbance at a particular energy near L<sub>III</sub>. The sample path length was established by cleaving the single crystal samples with the aid of adhesive tape, to achieve an optimum ratio of incident to transmitted intensities  $I_0/I$  near the edge such that the absorbance  $A \equiv \ln(I_0/I) \sim 2-3$ , corresponding to thicknesses of  $\approx 25 \mu\text{m}$ . The Ta mass absorption coefficients near the L edges are given in table 1, and are taken from the CRC handbook. The x-ray beam from a synchrotron is highly polarised in one direction  $E$  normal to the propagation vector  $k$ , which can be important in the interpretation of both the edge structure and the extended x-ray absorption fine structure (EXAFS) which we shall report later. In these experiments  $k$  is parallel to the crystal  $c$  axis and perpendicular to the TaS<sub>2</sub> or TaSe<sub>2</sub> layers for the dichalcogenide compounds. The instrumental resolution is better than 0.7 eV, which is the width at half-height of the silicon diffraction references in figures 2 and 3 (Acrivos *et al* 1980). Initial and final state lifetimes will decrease the resolution of the L edge measurements (Parratt 1959, Brown 1974). The width of a level of a particular symmetry increases monotonically with photon energy for the lighter elements (Parratt 1959) giving, by extrapolation, a full width at half height (FWHM) of  $\approx 6$  eV for the Ta L<sub>III</sub> level. This is in agreement with our data, for which the sharpest lines have a similar FWHM. Thus the short lifetimes of the Ta L levels limit the resolution of the experiments, so much so that fine features in the conduction band density of states (of total width  $\sim 7$  eV for the Ta dichalcogenides) cannot be observed. Note that in the soft x-ray region the FWHM is very much smaller, and in particular for the Se M<sub>V</sub> level is about 0.2 eV; but that, as mentioned previously, the interpretation of the absorption spectrum is more complicated at low energies because of overlap of absorption edges.

The applicability of the electromagnetic theory of absorption spectroscopy at x-ray energies has been examined by Rehn (1979). In the x-ray spectral region the real part of the refractive index  $n \approx 1$ , and the extinction coefficient  $\kappa \ll 1$ . Rehn (1979) has defined  $1 - n \equiv \delta$  and both  $\delta$  and  $\kappa$  decrease monotonically with the photon energy  $E$ , except near the x-ray absorption edge where quantum conditions are satisfied. It thus follows that  $\tilde{n}$  and  $\tilde{\epsilon}$  are given approximately by

$$\tilde{n} \equiv 1 - \delta + i\kappa \sim 1 \quad (1)$$

and

$$\tilde{\epsilon} \equiv n^2 - \kappa^2 + 2i n \kappa \approx 1 - 2\delta + 2i\kappa. \quad (2)$$

If interference effects may be neglected, the transmittance of our thin samples for incident light parallel to the  $c$  axis is given by the usual relation,

$$T(E) = \frac{I}{I_0} = \frac{(1 + \kappa^2/n^2)(1 - R_0)^2 \exp(-\bar{\mu}t)}{1 + R_0^2 \exp(-2\bar{\mu}t)} \quad (3)$$

where the reflectance  $R_0$  is given by

$$R_0(E) = \frac{(n-1)^2 + \kappa^2}{(n+1)^2 + \kappa^2} \approx \frac{\delta^2 + \kappa^2}{4} \quad (4)$$

in the above approximation and where  $\mu = 4\pi\kappa/\lambda$ , and  $\bar{\mu}$  is defined by

$$\bar{\mu} = \alpha_a(E)\rho_a t_a + \sum_{i \neq a} \alpha_i(E)\rho_i t_i = A_a + A_{bg} \quad (5.1)$$

where the  $\alpha(E)$  are experimental mass absorption coefficients (given, for example, in the Chemical Rubber Company handbook) for the matter in the x-ray path of length  $t$ , and  $\rho$  is the associated density. We distinguish the Ta atoms by the subscript  $a$ . Below the edge we define  $\alpha_a = \alpha_{a<}$  and above the edge  $\alpha_a = \alpha_{a>}$ , so that at the absorption edge  $E_a$  there is a discontinuity in  $\bar{\mu}$ , the so-called edge jump, given by

$$\Delta A = (\bar{\mu}_{>} - \bar{\mu}_{<})_{E_a} = (\alpha_{a>} - \alpha_{a<}) \rho_a t_a \quad (6)$$

where  $\Delta\alpha_a^0 = \alpha_{a>}^0 - \alpha_{a<}^0$  are given in table 1 for the three L edges for the elemental Ta standard. It follows from equations (3) and (4) that within the above approximation

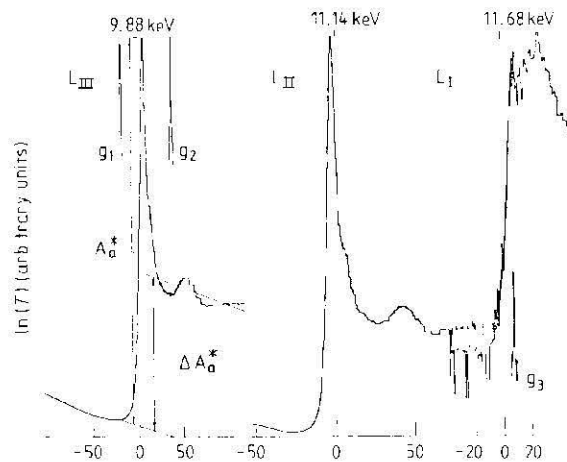
$$\bar{\mu} \approx \ln(I_0/I) \quad (5.2)$$

Figure 2 shows plots of transmittance against energy for a typical compound near the  $L_{\text{I}}$ ,  $L_{\text{II}}$  and  $L_{\text{III}}$  edges. Similar results are obtained for all the unintercalated compounds shown in table 2. From equation (5) it follows that

$$A = -\ln(T) = A_a(E) + A_{bg}(E) \quad (7)$$

where the background contribution  $A_{bg}$  can be subtracted out to obtain  $A_a(E)$  as follows:

$$A_a(E) = A_a^*(E) [1 - \chi_{as}(E)] \quad (8)$$



**Figure 2.** X-ray absorption spectra at the Ta L edges in 2H-TaS<sub>2</sub>, showing the peaks associated with transitions into conduction band states, seen superimposed on the edge jump.  $\Delta A_{a1}^*$ , the edge jump, is defined in the figure and  $A_{a1}^*$  is the magnitude of the superimposed peak. The results clearly show that the peak at the  $L_{\text{I}}$  edge is considerably smaller than that at the  $L_{\text{II}}$  or  $L_{\text{III}}$  edge, and indeed can only just be resolved.  $g_i$  are the Si diffraction peak energy reference markers. Note that the energy is given with respect to the absorption edge position in pure tantalum.

**Table 2.** I  
measurem  
are the lea  
and its siz

Compound

1T-TaS<sub>2</sub>

2H-TaS<sub>2</sub>

1T-TaSe<sub>2</sub>

2H-TaSe<sub>2</sub>

TaSc<sub>3</sub>

3R-TaS<sub>2</sub>

2H-TaS<sub>2</sub>

xTaSe<sub>2</sub>

(1T)

xTaSe<sub>2</sub>

(2H)

TaSc<sub>3</sub>

2H-TaS<sub>2</sub>

2H-TaS<sub>2</sub>

2H-TaS<sub>2</sub>

where  $A_a^*(E)$  correspon  
and continuum states ar

Additional peaks no  
2 are identified with tra  
measured with respect  
 $A_{a1}^*/\Delta A_{a1}^*$  are compare  
ratios for either the  $L_{\text{II}}$

1T-TaS<sub>2</sub>

**Table 2.** Intensities of the additional peaks seen near the absorption edges in the XAS measurements, measured with respect to the edge jump. Note that the L<sub>I</sub> edge measurements are the least reliable because the peak is of the same order of magnitude as the edge jump and its size will depend sensitively on its position with respect to the edge.

Compound	L edge	Run number	$A_{a1}^*/\Delta A_{a1}^*$
1T-TaS <sub>2</sub>	I	V208, 9	≅0.5
	II	V204	3.3
	III	V211	2.9
2H-TaS <sub>2</sub>	I	V225, 6	≅0.5
	II	V121, 1	3.1
	III	V152, 3	2.5
1T-TaSe <sub>2</sub>	I	V197	≅0.5
	II	V192, 3	3.1
	III	V168, 9	2.2
2H-TaSe <sub>2</sub>	I	V228, 9	≅0.5
	II	V234, 5	2.6
	III	V180, 2	1.8
TaSc <sub>3</sub>	I	V246, 7	≅0.5
	II	V139, 140	3.2
	III	V142	2.7
3R-TaS <sub>2</sub> · I <sub>43</sub>	I	VI205	≅0.6
	II	VI248	3.2
	III	VI204	3.2
2H <sub>r</sub> -TaS <sub>2</sub> · I <sub>23</sub>	I	VI236, 7	≅0.5
	II	VI216, 142	3.1
	III	VI208	2.9
xTaSc <sub>2</sub> · I <sub>x</sub> (1T)	I	VI238	≅0.5
	II	VI239	3.0
	III	VI177	1.9
xTaSc <sub>2</sub> · I <sub>x</sub> (2H)	I	VI240	≅0.5
	II	VI242, 3	3.2
	III	VI173, 5	1.6
TaSe <sub>3</sub> · I <sub>23</sub>	I	VI245, 6	≅0.3
	II	VI23, 4	3.5
	III	VI247	2.8
2H-TaS <sub>2</sub> · Cr <sub>13</sub>	I	VIM130	≅0.4
	II	—	—
	III	VIM123	2.2
2H-TaS <sub>2</sub> · Co <sub>13</sub>	I	VIM125	≅0.5
	II	VIM127	2.1
	III	VIM124	1.5
2H-TaS <sub>2</sub> · Ni <sub>13</sub>	I	VIM116	≅0.5
	II	—	—
	III	VIM117	2.4

where  $A_a^*(E)$  corresponds to transitions into bound (whether delocalised or localised) and continuum states and  $\chi_{as}$  defines the EXAFS contribution from the local environment.

Additional peaks near the absorption edges in the XAS measurements shown in figure 2 are identified with transitions to bound states. The intensities of these peaks,  $A_{a1}^*$ , are measured with respect to the edge jump  $\Delta A_{a1}^*$ , as shown in figure 2. The ratios  $A_{a1}^*/\Delta A_{a1}^*$  are compared for different Ta chalcogenides at a given edge in table 2. The ratios for either the L<sub>II</sub> or L<sub>III</sub> edges decrease in the following order:

$$1T\text{-TaS}_2 > \text{TaSc}_3 > 2H\text{-TaS}_2 \sim 1T\text{-TaSe}_2 > 2H\text{-TaSe}_2$$

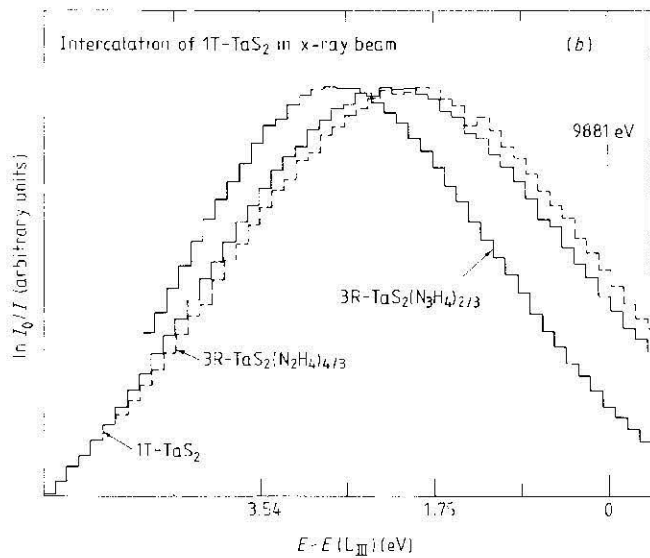
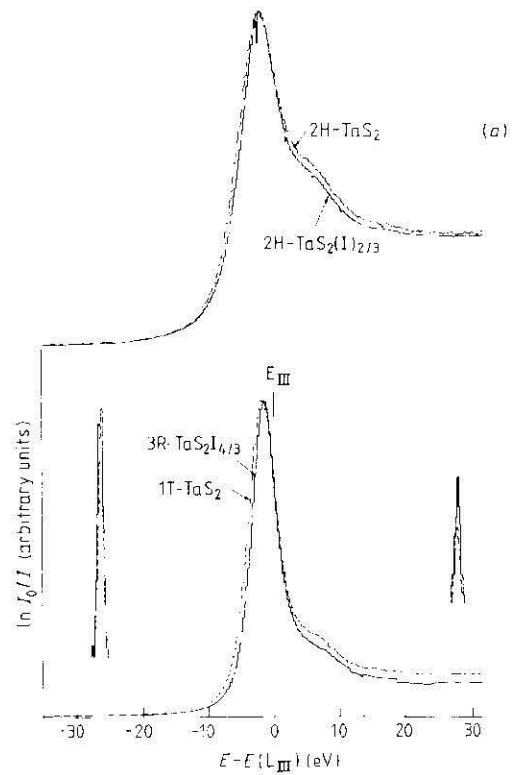


**Figure 3.** Changes in the Ta 4f XPS spectra resulting from the intercalation of 1T-TaS<sub>2</sub> by N<sub>2</sub>H<sub>4</sub> and N<sub>3</sub>H<sub>4</sub> resulting from the intercalation of 2H-TaS<sub>2</sub> before and after the intercalation of 1T-TaS<sub>2</sub>. Only small changes are observed at the energies near  $E_{III}$  in the spectra taken during the intercalation, clearly indicating the presence of 1T-TaS<sub>2</sub>. The intercalation of 1T-TaS<sub>2</sub> in the 2H-TaS<sub>2</sub> layers per Ta atom is clearly indicated by the two intercalation peaks at  $E_{III}$  on pumping, suggesting the presence of 1T-TaS<sub>2</sub> in the intercalated structure (see also the infrared transmission spectra of the intercalated 2H-TaS<sub>2</sub> and 1T-TaS<sub>2</sub> and the Ta 4f XPS spectra of the intercalated 2H-TaS<sub>2</sub> and 1T-TaS<sub>2</sub> selenides and tellurides). The shoulder at  $E_{III}$  in the Ta 4f XPS spectra is due to the intercalation of 1T-TaS<sub>2</sub> in the 2H-TaS<sub>2</sub> layers as a shoulder.



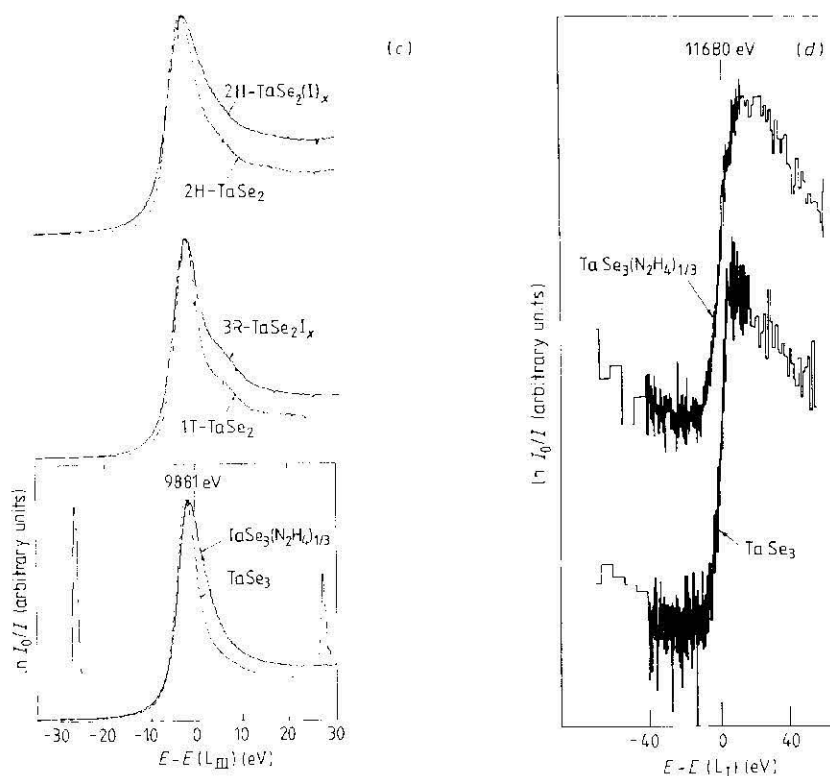


**Figure 3.** Changes in the Ta L edge x-ray absorption spectra in several Ta chalcogenides, resulting from hydrazine ( $N_2H_4$ ) intercalation. (a) XAS at the Ta L<sub>III</sub> edge in 1T-TaS<sub>2</sub> and 2H-TaS<sub>2</sub> before and after intercalation with hydrazine. Note that the intercalation causes only small changes in the spectra of these sulphides. (b) A detail of the L<sub>III</sub> edge XAS for energies near the peak position for intercalation of 1T-TaS<sub>2</sub>. More than 40 spectra were taken during and prior to intercalation of 1T-TaS<sub>2</sub> with  $N_2H_4$  to form 3R-TaS<sub>2</sub>( $N_2H_4$ )<sub>4/3</sub>, clearly indicating that the peak position is shifted to higher energies in 3R-TaS<sub>2</sub>( $N_2H_4$ )<sub>4/3</sub>. The intercalation complex formed in this way, 3R-TaS<sub>2</sub>( $N_2H_4$ )<sub>4/3</sub>, contains two intercalate layers per TaS<sub>2</sub> layer (Acrivos 1979). Pumping on the intercalated sample removes one of the two intercalate layers to give 3R-TaS<sub>2</sub>( $N_2H_4$ )<sub>2/3</sub> (Acrivos 1979). The XAS spectra obtained on pumping, shown in the figure, indicates that the peak position is shifted to lower energies in the intercalation complex, 3R-TaS<sub>2</sub>( $N_2H_4$ )<sub>2/3</sub>, even as compared with the unintercalated host compound, 1T-TaS<sub>2</sub>. The signs of the shifts are consistent with the changes seen in the infrared transmission spectra, induced by hydrazine intercalation (M Sarma private communication). (c) XAS spectra at the Ta L<sub>III</sub> edge before and after intercalation of 1T-TaS<sub>2</sub>, 2H-TaSe<sub>2</sub> and TaSe<sub>3</sub> with  $N_2H_4$ . Note that much larger changes are seen in the spectra of the Ta selenides as compared to the Ta sulphides (see figures 3(a) and 3(b)). (d) XAS spectra at the Ta L<sub>I</sub> edge in TaSe<sub>3</sub>, showing a significant change in the magnitude of the L<sub>I</sub> peak induced by intercalation. The peak can be seen above the edge jump in the pure compound, but only as a shoulder in the intercalated material.

in rough agreement with the order expected from chemical arguments. On intercalation with  $N_2H_4$  the ratio decreases for the three selenides but it increases for the disulphides. However, for the Cr, Co and Ni intercalates of 2H-TaS<sub>2</sub>, the ratio is decreased in all cases with the greatest change observed for the Co intercalate. These results will be presented in more detail in a separate publication.

The oscillator strengths can be compared by taking into account the dependence of  $\Delta A_a^*$  on  $\Delta \alpha_a^0$  through equation (6). Given

$$\Delta \alpha_a^0 \rho_a t_a \propto M_a^0 |^2 / E_a^2 \quad (9)$$

where  $M_a^0$  is the matrix element for the transition probability from the L core states to the continuum (in pure tantalum), excluding transitions to bound states, it follows that

$$N_c |M_a|^2 \propto \Delta \alpha_a^0 E_a^2 (A_{a1}^* / A_a^*) \quad (10)$$

where  $N_c$  is the density of final states and  $M_a$  the matrix element for the transition probability from the corresponding L core state to conduction band states. Using relation (10) we have estimated the relative amount of p-d character in the final states using the relation

$$r_i = \frac{(N_c |M_a|^2)_{p\text{states}}}{(N_c |M_a|^2)_{d\text{states}}} = \frac{\Delta \alpha_{ai}^0 E_i^2 (A_{a1}^* / \Delta A_a^*)_i}{\Delta \alpha_{ai}^0 E_i^2 (A_{a1}^* / \Delta A_a^*)_i} \quad (11)$$

where  $i = \text{II}$  or  $\text{III}$ . We now define the percentage p character of the final states as seen in this experiment by the following:

$$p_i = 100r_i / (1 + r_i). \quad (12)$$

Using the values  $\Delta \alpha_{ai}^0 E_i^2 = 5.87 \times 10^3$ ,  $8.69 \times 10^3$  and  $14.54 \times 10^3 \text{ cm}^2 \text{ g}^{-1} (\text{keV})^2$  for the L<sub>I</sub>, L<sub>II</sub> and L<sub>III</sub> edges respectively and values for  $A_{a1}^* / \Delta A_a^*$  given in table 2 via relation (11), we find that  $p_{\text{II}}$  and  $p_{\text{III}}$  are similar and lie in the range 6–10%.

In order to compare these results with band structure calculations the nature of the transition moments must be examined. The matrix element  $M_a$  for the transition can be written as a product of a term which depends only on the symmetry of the initial and final states and a term which depends on the spatial distributions of these states (Wigner-Eckart theorem). The symmetry-dependent term will, in principle, depend on the direction of the radiation field  $E$  (see for example Tinkham 1964) and therefore the p-d character given in table 2 refers only to the symmetry-allowed transitions under the particular conditions of the experiment (namely  $E$  parallel to the TaS<sub>2</sub> or TaSe<sub>2</sub> layers for the dichalcogenides ( $k \parallel c$ )). When the final state is a hybrid of contributions from different states and the initial state is centred at only one atom, in this case Ta, then the contributions to  $M_a$  will be weighted by the overlap of the initial state with the hybrid components of the final state. Thus the p character given by relation (12) is a measure of the Ta p character in the conduction band plus a small contribution due to overlap with chalcogen states, not necessarily of p character. Therefore it follows that the total p character of the band is larger than that reported above.

Although in practice insufficient flux is available at the SSRL, in principal similar measurements at the chalcogen L edges would reveal the amount of chalcogen p character in the conduction band together with some contribution due to overlap of the initial state with states centred on the Ta atoms. (In 2H NbSe<sub>2</sub> we estimate the contribution due to overlap with the transition metal atom to be about 10% from the overlap of the Nb 4d and Se p $\sigma$  states of 0.31 calculated by Doran *et al* 1978.) Thus it would be

possible to determine band from measurements.

The conduction band character, although it is between 6 and 10%. This is in the conduction band optical spectra. For example unoccupied higher-energy bands may be the case if the interpretation of the transition metal intercalation is correct.

There are interesting features in the conduction band is red shifted (see table 3). Moreover, in this case the shift is such. Such a shift could be due to charge transfer from the transition to lower energy states which shifts the transition to lower energy. The conduction band hybridisation of the band.

We thank A R Beal for helpful discussions at SJSU and NSF DM Energy, and a NATO grant which edges a travel grant from

## References

- Acrivos J V 1979 *Physics and Chemistry of Intercalation* (Dordrecht: Reidel)
- Acrivos J V *et al* 1980 *Stanford University Report*
- Bell M G and Liang W Y 1979 *Phys. Rev. B* **20**, 1000
- Brown F C 1974 *Solid State Chemistry* vol 29
- Doran N J 1980 *Proc. Int. Conf. on Intercalation* (London: Taylor & Francis)
- C Haas and H W Myron 1979 *Phys. Rev. B* **20**, 1000
- Doran N J, Ricco B, Titterton J, Goldberg A M, Beal A R, Liang W Y and Beal A R 1979 *Phys. Rev. B* **20**, 1000
- Lindau I and Winick H 1976 *Phys. Rev. Lett.* **36**, 215
- Parkin S S P and Beal A R 1979 *Phys. Rev. B* **20**, 1000
- Parratt L G 1959 *Rev. Mod. Phys.* **31**, 633
- Rehn 1979 *SSRL Report*
- Sonntag B and Brown F C 1979 *Phys. Rev. B* **20**, 1000
- Tinkham M 1964 *Group Theory and Physics* (New York: McGraw-Hill)
- Winick H and Brown G (ed) 1979 *Phys. Rev. B* **20**, 1000

possible to determine a maximum value for the amount of p character in the conduction band from measurements at the chalcogen and metal L edges.

The conduction band in the Ta chalcogenides studied has a significant amount of p character, although it has only been possible to deduce a lower limit on this amount of between 6 and 10%. These are the first direct measurements of the extent of p character in the conduction band of these compounds and may assist in the interpretation of their optical spectra. For example, transitions between occupied conduction band states and unoccupied higher-energy band states of d character are not forbidden as would otherwise be the case if the conduction band were purely of d symmetry, which supports the interpretation of the reflectivity spectra of the group V(a) dichalcogenides and their 3d transition metal intercalates given by Parkin and Beal (1980).

There are interesting effects on intercalation. For example, the Ta p character of the conduction band is reduced in going from  $\text{TaSe}_3$  to  $\text{TaSe}_3(\text{N}_2\text{H}_4)_{1/3}$  (see table 2 and figure 3). Moreover, in this compound the  $L_{\text{III}}$  edge is shifted to higher energies on intercalation. Such a shift could be the result of two competing effects: (i) shielding of the core levels by charge transfer from the intercalate to the conduction band which would shift the transition to lower energy; and (ii) filling of the conduction band through charge transfer which shifts the transition to higher energies. Thus it appears that intercalation modifies the conduction band not only through charge transfer but also through changes in hybridisation of the band.

We thank A R Beal for providing crystals and are grateful to A D Yoffe and W Y Liang for helpful discussions. This work was partly supported by contracts NSF DMR7910011 at SJSU and NSF DMR7727489 at SSRL in cooperation with the US Department of Energy, and a NATO grant 1441 at the Cavendish Laboratory. S S P Parkin acknowledges a travel grant from Trinity College, Cambridge.

### References

- Acrivos J V 1979 *Physics and Chemistry of Materials with Layered Structures: Intercalated Layer Materials* ed F Levy (Dordrecht: Reidel) p 94
- Acrivos J V et al 1980 *Stanford Synchrotron Radiation Laboratory Report*
- Bell M G and Liang W Y 1976 *Adv. Phys.* **25** 53
- Brown F C 1974 *Solid State Physics* ed H Ehrenreich, F Seitz and D Turnbull (New York: Academic Press) vol 29
- Doran N J 1980 *Proc. Int. Conf. on Layered Materials and Intercalates, Nijmegen 1979* ed C F van Bruggen, C Haas and H W Myron (Amsterdam: North-Holland)
- Doran N J, Ricco B, Titterton D J and Wexler G 1978 *J. Phys. C: Solid State Phys.* **11** 685
- Goldberg A M, Beal A R, Levy F A and Davis E A 1975 *Phil. Mag.* **32** 367
- Liang W Y and Beal A R 1976 *J. Phys. C: Solid State Phys.* **9** 2823
- Lindau I and Winick H 1976 *Scientific and Industrial Applications of Small Accelerators, Fourth Conference* 1976 p 215
- Parkin S S P and Beal A R 1980 *Phil. Mag.* **42** 627
- Parratt L G 1959 *Rev. Mod. Phys.* **31** 616
- Rehn 1979 *SSRL Report*
- Sonntag B and Brown F C 1974 *Phys. Rev.* **B10** 2300
- Tinkham M 1964 *Group Theory and Quantum Mechanics* (New York: McGraw-Hill)
- Winick H and Brown G (ed) 1978 *Stanford Synchrotron Radiation Laboratory Report no 78/04*.